

# Delafloxacin-Loaded Poly(D,L-lactide-co-glycolide) Nanoparticles for Topical Ocular Use: *In Vitro* Characterization and Antimicrobial Activity

Abdullah K. Alshememry, Mohd Abul Kalam, Mudassar Shahid, Raisuddin Ali, Sulaiman S. Alhudaithi, Nada A. Alshumaimeri, Ziyad A. BinHudhud, Abdulrazzaq A. Aldaham, Ziyad Binkhathlan, and Aliyah A. Almomen\*



Cite This: *ACS Omega* 2024, 9, 50476–50490



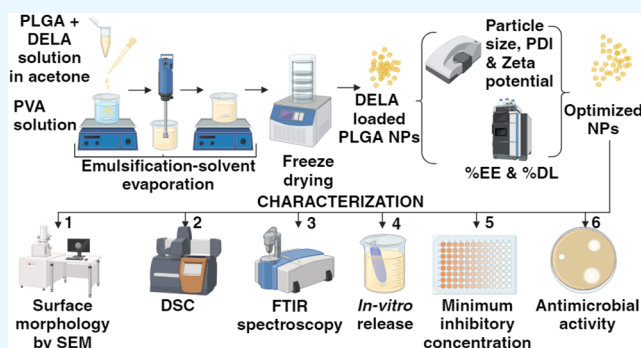
Read Online

ACCESS |

Metrics & More

Article Recommendations

**ABSTRACT:** **Objective:** We developed delafloxacin (Dela)-loaded PLGA nanoparticles (PNPs) for potential ocular application *via* a topical route to treat eye infections caused by Gram-positive and Gram-negative bacteria. **Methodology:** Dela-PNPs were formulated using the emulsification-solvent evaporation method and stabilized using poly(vinyl alcohol) (PVA). Size and morphology were characterized by using dynamic light scattering (DLS) and scanning electron microscopy (SEM). Drug loading and encapsulation efficiency were measured *via* HPLC. Differential scanning calorimetry (DSC) and Fourier-transform infrared spectroscopy (FTIR) assessed the physical state and drug–polymer interaction. The *in vitro* drug release was evaluated using the dialysis bag method in simulated tear fluid (STF, pH 7.4) with Tween 80 (0.5%). The antimicrobial efficacy was determined by a minimum inhibitory concentration (MIC) and zone of inhibition tests against various bacteria. **Results:** Optimally sized PNPs were produced ( $238.9 \pm 10.2$  nm) with a PDI of  $0.258 \pm 0.084$  and a  $\zeta$ -potential of  $2.78 \pm 0.34$  mV. Using 40 mg of PLGA, 4 mg of Dela, and 1% PVA, drug encapsulation and loading were  $84.6 \pm 7.3$  and  $12.9 \pm 1.7\%$ , respectively. DSC indicated that Dela was entrapped in an amorphous state within the PNPs. FTIR spectra showed no drug–polymer interactions. The formulation showed  $40.6 \pm 4.2\%$  drug release within 24 h and  $84.4 \pm 6.1\%$  by 96 h. MIC tests showed high susceptibility of *Streptococcus pneumoniae*, *Klebsiella pneumoniae*, and *Escherichia coli* ( $\sim 0.31$   $\mu\text{g}/\text{mL}$ ) compared to *Staphylococcus aureus* and MRSA-6538 ( $\sim 0.63$   $\mu\text{g}/\text{mL}$ ) and *Bacillus subtilis* ( $2.5$   $\mu\text{g}/\text{mL}$ ). Stability studies showed minimal changes in particle characteristics over 3- and 6-month storage at 25 and 37 °C. **Conclusion:** Dela-PNPs exhibit significant potential as a nanof ormulation for ocular applications.



## 1. INTRODUCTION

Delafloxacin (Dela) is a recently developed fluoroquinolone antibiotic that received approval from the US FDA in 2017.<sup>1</sup> Its chemical designation is 1-(6-amino-3,5-difluoropyridin-2-yl)-8-chloro-6-fluoro-7-(3-hydroxyazetidin-1-yl)-4-oxoquinoline-3-carboxylic acid with a molecular weight of 440.8 g/mol. The molecular structure of Dela is shown in Figure 1. This anionic fluoroquinolone is effective against a wide range of pathogens, including those responsible for “acute bacterial skin and skin structure infections (ABSSSIs).”<sup>2–4</sup> Being an anionic fluoroquinolone that acts equally against Gram-positive and Gram-negative pathogenic bacteria, it exerts its effects through dual-targeted inhibition of essential bacterial enzymes, including DNA gyrase (topoisomerase-II) and topoisomerase-IV. Dela exhibits a distinct binding affinity to these enzymes compared to other fluoroquinolones (such as

ciprofloxacin, levofloxacin, and trovafloxacin), resulting in enhanced inhibition of both topoisomerase-II and topoisomerase-IV, 2.<sup>5–8</sup> It is indicated for treating community-acquired respiratory tract infections and is currently being evaluated in clinical trials for similar applications.<sup>9,10</sup> Following oral administration, Dela is quickly absorbed, reaching peak plasma concentrations within 1–2.5 h;<sup>11</sup> however, its poor aqueous solubility results in a relatively low absolute oral bioavailability of 58.8%.<sup>12</sup>

**Received:** August 24, 2024  
**Revised:** October 8, 2024  
**Accepted:** November 28, 2024  
**Published:** December 12, 2024



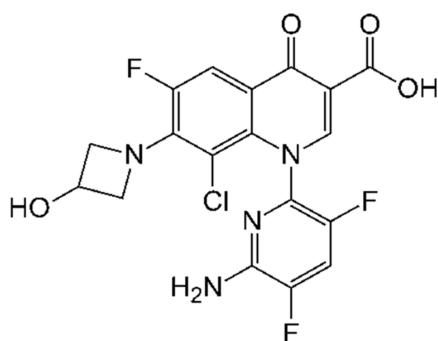


**Figure 1.** Molecular structure of delafloxacin ( $C_{18}H_{12}ClF_3N_4O_4$ ).

Due to rapid metabolism (half-life of  $\leq 2.5$  h) and low absolute bioavailability, frequent administration of conventional dosage forms of Dela might be needed even as topical use for the treatment of eye infections. There is limited ocular availability of drug(s) *via* topical ocular application of conventional dosage forms due to low corneal permeability caused by the physiological barrier and defensive mechanism of the eye structures (*i.e.*, distinctive outer epithelial, middle stroma, and inner endothelial layers), blinking of the eyelids, rapid tear dilution, and other factors.<sup>13–15</sup> The ocular physiological barrier is also supplemented by the physicochemical barrier of the mucin layer that restricts the ocular uptake of drug(s)/antigen(s).<sup>14</sup> Consequently, free drug solutions (conventional ocular dosage forms) are eliminated from the ocular surfaces immediately after dosing, and only around 5–7% of the administered dose is actually available to the intraocular tissues.<sup>15–18</sup> To achieve a therapeutic concentration of applied drugs, recurrent dosing is needed, which can be a reason for adverse drug reactions and patient noncompliance.<sup>19</sup> These facts encouraged us to develop a nanocarrier for the ocular delivery of Dela that would provide prolonged drug release to intraocular tissues.

Among the nanocarriers such as lipid nanocarriers,<sup>20,21</sup> microemulsions,<sup>13</sup> bilosomes,<sup>7,18</sup> chitosan-based nanoparticles,<sup>16,22</sup> poly(D,L-lactide-co-glycolide, 50:50 D,L-lactide: glycolide or PLGA) based nanoparticles (PNPs) have gained popularity for the targeted and controlled ocular drug delivery carrier of numerous therapeutic agents.<sup>8,13,23</sup> The preparation of PLGA-based NPs makes it easier to get the smaller-sized uniform particles with efficient drug encapsulation as compared to the above nanocarriers. Moreover, because of their smaller size and solid spherical structures, PNPs are very effective for the delivery and targeting of drugs, as the NPs can easily diffuse across the ocular cells, penetrate the bacterial cells, and interfere with their vital molecular pathways, thus providing an exceptional antimicrobial mechanism. PLGA, a US-FDA-approved synthetic copolymer, is biocompatible and biodegradable, and its nanoparticle acts as a potential carrier system for superior interaction with biological membranes. After thoroughly reviewing the available literature, we found that very limited work has been reported until now to improve the ocular bioavailability of Dela using PNPs as carriers by increasing the drug concentration across the eye structures.

With this in mind, we developed Dela-loaded PNPs by a double emulsion-solvent evaporation method and characterized them in terms of particle size, size distribution, and surface charge by Zetasizer. The structural morphology of the optimal formulation was examined by scanning electron microscopy. The drug encapsulation and loading in PNPs were estimated.

Differential scanning calorimetry and Infrared spectroscopy were performed to see the amorphous state of the loaded drug into NPs. *In vitro* release of Dela from the optimal PNPs as compared to Dela aqueous suspension was performed in simulated tear fluid (pH 7.4), and the kinetics of drug release was investigated. The sterility testing of the optimal Dela-PNP suspension was done, the minimum inhibitory concentration of Dela-PNPs was determined, and the antimicrobial potential was determined against certain Gram-positive and Gram-negative bacterial strains to confirm the ophthalmic suitability of the developed formulation.

## 2. MATERIALS AND METHODS

**2.1. Materials.** Delafloxacin (purity  $\geq 98\%$ ,  $C_{18}H_{12}ClF_3N_4O_4$ ;  $M_w$ : 440.8 g/mol,  $\log P$ : 2.7) was purchased from “Amadis Chemical Company Ltd. Zhejiang, China”. Poly(D,L-lactide-co-glycolide), 50:50 D,L-lactide:glycolide (PLGA,  $M_w$ : 30,000–60,000), poly(vinyl alcohol) (PVA 87–90% hydrolyzed,  $M_w$ : 30,000–70,000), and hydrochloric acid (HCl, Ph. Eur. Fuming  $\geq 37\%$ ) were purchased from Sigma-Aldrich Co. (St. Louis, MO). Tween 80 was purchased from Eurostar Scientific Ltd., Liverpool, U.K. Methanol (HPLC grade) was purchased from “BDH Ltd. (Poole, England)”. Acetonitrile, CHROMASOLV, gradient grade, for HPLC  $\geq 99.9\%$  was purchased from Sigma-Aldrich Lab., GmbH, Germany. An in-house Milli-Q purifying system (Millipore, France) was used to obtain purified water. All other chemicals and solvents were of analytical grade and used as obtained without further purification.

**2.2. Preparation of PLGA-Based Nanoparticles (PNPs).** Polymeric nanoparticles (PNPs) were synthesized using an emulsification-solvent evaporation technique.<sup>13,24</sup> To begin, 40 mg of polymer (PLGA) was precisely weighed and dissolved in 2.5 mL of acetone, forming the organic phase. Various concentrations of poly(vinyl alcohol) (PVA), serving as a stabilizer, were prepared by dissolving specific amounts of PVA in Milli-Q water, creating the aqueous phase (with concentrations of 0.25, 0.5, and 1%, w/v). The organic phase (2.5 mL) was gradually introduced into the aqueous phase (7.5 mL) under continuous magnetic stirring at 800 rpm and homogenized at 21,500 rpm for 15 min to form a primary emulsion. Subsequently, a larger volume of the aqueous phase (approximately 3 times the volume of the primary emulsion) was slowly added to the emulsion while maintaining magnetic stirring. This process led to the formation of organic phase droplets. The magnetic stirring was sustained for 4 h to evaporate the excess organic solvent (acetone), resulting in a suspension of blank PLGA nanoparticles (PNPs).

In a similar manner, delafloxacin (Dela)-loaded PLGA nanoparticles (Dela-PNPs) were prepared by dissolving 4 mg of Dela in the organic phase, maintaining a drug/polymer ratio of 1:10 (w/w); the remaining steps followed the procedure described above. The suspended PNPs were purified by washing with Milli-Q water (3 times) using ultracentrifugation at 30,000 rpm for 25 min at 4 °C to eliminate any residual surfactant or stabilizer. After the final wash, the PNP pellets were collected, redispersed in 10 mL of Milli-Q water, and freeze-dried. The freeze-dried formulations were stored in a refrigerator until needed for further studies. For comparison, an aqueous suspension of Dela (Dela-AqS) was prepared by suspending 10 mg of the drug in 10 mL of normal saline containing 0.003% (w/v) phenyl mercuric nitrate as a

preservative.<sup>13,25</sup> In the Del-AqS, 0.25% (w/v) Tween 80 was added to increase the aqueous solubilization of the drug.

**2.3. Chromatographic Analysis of Dela.** For the analysis of delafloxacin (Dela), a reverse-phase high-performance liquid chromatography (HPLC) method with ultraviolet (UV) detection was employed based on a previously reported procedure with minor adjustments.<sup>26,27</sup> The HPLC system used was a Waters 1500-series controller equipped with a UV detector (Waters Model 2489), a binary pump (Waters Model 1525), and an automated sampling system (Waters Model 2707 Autosampler). The system's operation and data processing were managed using "Breeze software". A sample volume of 20  $\mu$ L was injected into the analytical column, which was a C<sub>18</sub> column (Macherey-Nagel, 150  $\times$  4.6 mm<sup>2</sup>, 5  $\mu$ m) maintained at 60 °C in the column oven. The mobile phase consisted of a 50:50 (v/v) mixture of acetonitrile and Milli-Q water with 0.2% hydrochloric acid, adjusted to a pH of 3.5. This was pumped isocratically at a flow rate of 1 mL/min, with a total run time of 7 min. The drug, Dela, was eluted at approximately 3.25  $\pm$  0.51 min, and UV detection was performed at 290 nm ( $\lambda_{\text{max}}$ ).

**2.4. Characterization and Structural Morphology of PNPs.** The characterization of delafloxacin-loaded polymeric nanoparticles (Dela-PNPs), including size, polydispersity index (PDI), and  $\zeta$ -potential, was conducted using the dynamic light scattering (DLS) technique, utilizing a Zetasizer Nano-Series instrument (Nano-ZS, Malvern Inc. Ltd., United Kingdom). The system was operated at a detection angle of 90° and a temperature of 25 °C. Before each measurement, the PNPs were suspended and diluted (1:10, v/v) with a mixture of Milli-Q water, which has a dielectric constant of 78.5.  $\zeta$ -Potential measurements were performed using the same instrument under identical conditions. All measurements were carried out in triplicate.

The structural and surface morphology of the PNPs were analyzed through scanning electron microscopy (SEM) using a Zeiss EVO LS10 (Cambridge, U.K.). The SEM analysis was conducted using the standard gold-sputter technique to enhance imaging and morphological assessment. The nanoparticles were coated with gold by an "Ion-Sputter" at 20 mA current for 1 min prior to scanning. The scanning was then performed at an accelerating voltage of 20 kV, with a working distance (WD) of 6.5–8.5 mm and at a magnification of 50 KX.

**2.5. Encapsulation and Drug-Loading Efficiencies.** The encapsulation and loading of delafloxacin (Dela) in polymeric nanoparticles (PNPs) were assessed using an indirect method, which involved determining the amount of untrapped drug. This was done by calculating the differences between the initial drug amount used to prepare the Dela-PNPs and the amount of drug quantified in the supernatant (as described below). Accurately measured 10 mL of Dela-PNP suspension was vortexed and centrifuged (for 5 min at 12,000 rpm). A 20  $\mu$ L sample of the supernatant was then injected into the HPLC-UV system for Dela analysis, as previously described. The encapsulation efficiency and drug loading were subsequently calculated using the following eqs (eqs 1 and 2)

$$\%EE = \left( \frac{\text{amount of Dela used in PNPs} - \text{amount of Dela in the supernatant}}{\text{amount of Dela used in PNPs}} \right) \times 100 \quad (1)$$

$$\%DL = \left( \frac{\text{amount of Dela used in PNPs} - \text{amount of Dela in the supernatant}}{\text{total amount of Dela PNPs}} \right) \times 100 \quad (2)$$

**2.6. Differential Scanning Calorimetry.** Differential scanning calorimetry (DSC) was employed to analyze the physical state and thermal behavior of pure delafloxacin (Dela), polymer (PLGA), a physical mixture (PM) of Dela and PLGA, and freeze-dried Dela-loaded polymeric nanoparticles (Dela-PNPs). This analysis was performed by using a DSC-8000 instrument from PerkinElmer Instruments (Shelton, CT). The DSC measurements were conducted under an inert nitrogen atmosphere, with a nitrogen flow rate of 20 mL/min and a heating rate of 10 °C/min. The temperature range scanned was between 50 and 300 °C. Approximately 4–5 mg of each test sample was placed into aluminum pans, which were then sealed with lids for analysis. A similar unfilled pan was used as the reference in the DSC instrument. The resulting thermograms for all of the samples were recorded and analyzed using the "PYRIS Version-11" software, which is integrated with the DSC instrument.

**2.7. Fourier Transformed Infrared (FTIR) Spectroscopy.** Fourier-transform infrared (FTIR) spectroscopy was conducted on pure Dela, PLGA, the physical mixture (PM), and Dela-PNPs using a BRUKER Optik GmbH (Model Alpha, Germany) instrument. This technique was used to assess potential drug–polymer interactions and, to some extent, the physical state of the encapsulated drug. Approximately 4–5 mg of each sample was placed on the instrument's holder plate and exposed to infrared light. The IR spectra of all samples were recorded using the "OPUS V-7.8" software, which recorded the IR spectra of all of the samples from wavenumber 4000 to 400 cm<sup>-1</sup> at a resolution of 2 cm<sup>-1</sup>.

**2.8. In Vitro Drug Release and Release Kinetics.** A comparative *in vitro* release study was conducted to evaluate the release profiles of the pure drug suspension (Dela-AqS) and optimized drug-loaded polymeric nanoparticles (Dela-PNPs). The study was carried out using a dialysis membrane with a molecular weight cutoff of 12–14 kDa (Spectra/Por Dialysis Membrane, Spectrum Laboratories, Inc., Rancho Dominguez, CA). In brief, 1 mL of either Dela-AqS or the nanosuspension of Dela-PNPs was placed into separate dialysis bags, with both ends of the bags securely closed using Spectra/Por Weighted Closures. The suspensions were prepared in phosphate buffer (pH 7.4) with a drug concentration of 1000  $\mu$ g/mL. The dialysis bags were then placed into separate beakers containing 50 mL of simulated tear fluid (STF, pH 7.4 with 0.5% w/v Tween 80) as the release medium. The entire setup was maintained at 35  $\pm$  1 °C (mimicking ocular physiological temperature) in a shaking water bath (100 strokes per minute). At predetermined time intervals, 1 mL of the sample was withdrawn, and the same volume of prewarmed (at 35  $\pm$  1 °C) fresh release medium (STF, pH 7.4 with 0.5% w/v Tween 80) was added to maintain a constant volume and sink conditions. The drug content in the collected samples was analyzed using the HPLC-UV method previously described. The percentage of drug released (%DR) was calculated using the following equation (eq 3), and the amount of drug released (%) was plotted against time (h).

$$\begin{aligned} \%DR = & \\ & \frac{\text{conc. } (\mu\text{g/mL}) \times \text{DF} \times \text{vol. of release medium (mL)}}{\text{initial amount of Dela used } (\mu\text{g})} \\ & \times 100 \end{aligned} \quad (3)$$

The release data were fitted into various kinetic models, including zero-order, first-order, Korsmeyer–Peppas, Higuchi-matrix, and Hixson–Crowell models. The best-fit model for Dela release from the PLGA NPs was determined based on the highest correlation coefficient ( $R^2$ ) value, which approached 1.00. From the slope values, the release exponent ( $n$ -values) and other kinetic parameters were calculated to determine the order of reaction and the mechanism of drug release.<sup>16,28</sup>

**2.9. Antimicrobial Studies.** **2.9.1. Sterilization and Sterility Testing of Dela-AqS, Blank PNPs, and Dela-PNPs.** The formulations intended for microbiological use were prepared in an aseptic environment, following the guidelines for the aseptic filling method applicable to eye preparations.<sup>29</sup> The freeze-dried polymeric nanoparticles (PNPs) were sterilized by exposure to UV radiation (254 nm) for 3 h. After sterilization, the product was dispersed in water for injection and packed in sterile glass vials. The Dela aqueous suspension (Dela-AqS) was also prepared in the aseptic area using water for injection.

Sterility evaluation is a crucial quality control test for ophthalmic and parenteral products. In this study, sterility testing of the sterilized products was conducted according to the USP method.<sup>29,30</sup> Two containers of each sterilized product were used for the test. Approximately 2 mL of each product from the two containers was pooled under aseptic conditions and further diluted with 8 mL of water for injection. A sterile membrane filter with a 0.22  $\mu\text{m}$  pore size (Corning Inc., New York, NY 14831) was placed in the membrane-filter funnel unit. The membrane filter was premoistened with sterilized Fluid-A (0.1% w/v of Peptone). The diluted pooled samples were then passed through membrane filters. Since the products contained antimicrobial drugs, the membrane filters were washed 4 times with Fluid-A.

Subsequently, the membrane filters were divided into two pieces. One piece was placed into autoclaved “Soybean Casein Digest Media” or “Tryptone Soya Broth (TSB)” (for fungi/molds and lower bacteria) and incubated for 14 days at 20–25 °C. The other piece was placed into sterilized “Fluid Thioglycollate Media (FTM)” (for anaerobic and/or aerobic microorganisms) and incubated for 14 days at 30–35 °C. The absence of any microbial growth was confirmed by the presence of a clear, transparent solution/suspension.

**2.9.2. Minimum Inhibitory Concentration (MIC) Determination.** The minimum inhibitory concentrations (MICs) of an antibacterial drug against a specific microorganism are defined as the lowest concentration (or highest dilution) of the drug that inhibits the visible growth of the microorganism after at least 12 h of incubation. The MICs of delafloxacin (Dela) were determined against various Gram-positive bacteria, including *Staphylococcus aureus*, *Bacillus subtilis*, *Streptococcus pneumoniae*, and a methicillin-resistant *S. aureus* (MRSA) strain (SA-6538), as well as Gram-negative pathogens such as *Escherichia coli* and *Klebsiella pneumoniae*. The test was performed using an Iso-Sensitest agar medium, which contains stabilized minerals to prevent the antagonistic effects of metal ions on antimicrobials. This medium supports the growth of most microorganisms without the need for additional supplements. Dela (4 mg) was

dissolved in 200  $\mu\text{L}$  of DMSO, and then the final volume was made up to 10 mL with sterile Milli-Q water to get 400  $\mu\text{g/mL}$  drug concentration (stock solution). The stock solution was further diluted with sterile water to obtain a range of drug concentrations (20–0.156  $\mu\text{g/mL}$ ). The highest used concentration was 20  $\mu\text{g/mL}$ , which contained only 1  $\mu\text{L}$  of DMSO in 1 mL of 20  $\mu\text{g/mL}$  drug solution (0.1% DMSO, v/v). This small volume of DMSO in 1 mL of drug solution was negligible, as the maximum tolerable limit of DMSO in MICs determination is 0.5% v/v, i.e., 5  $\mu\text{L/mL}$ .<sup>31</sup>

Equivalent concentrations of Dela were prepared by suspending the appropriate amount of Dela-PNPs. The aqueous suspension of Dela-PNPs was prepared by suspending 10 mg of the drug in 10 mL of normal saline without a preservative.

Blank nanoparticles (B-PNPs) were also prepared similarly without adding the drug. In 96-well plates, 100  $\mu\text{L}$  of each drug product (solution and PNP suspension) was accurately measured and added to each well. Then, 100  $\mu\text{L}$  of  $1 \times 10^5$  CFU/mL suspension of the tested pathogens were transferred into each well. The addition of the pathogen suspension further diluted the drug products, resulting in a final concentration range of 10–0.078  $\mu\text{g/mL}$  of Dela. The plates were then incubated at 37 °C for 24 h. Visual inspection for turbidity in the wells was conducted with the MIC being the lowest concentration of Dela that completely inhibited microbial growth, indicated by a clear, transparent well.

**2.9.3. Antibacterial Activity by Zone of Inhibition Assay.** The antimicrobial activity of delafloxacin in Dela-PNPs and Dela-AqS (as a control preparation) was assessed using the agar diffusion method.<sup>22,32</sup> Based on the “Global Priority Pathogens List”, various Gram-positive and Gram-negative ATCC standard bacterial strains were obtained from the Microbiology Unit, Department of Pharmaceutics, College of Pharmacy, King Saud University, Riyadh, to evaluate their susceptibility to Dela. Each bacterial strain was spread on separate Mueller-Hinton agar plates. After 45 min, three wells with a diameter of 6 mm were created on each plate using a sterile borer. In well-1, 100  $\mu\text{L}$  of Dela-AqS (containing 50  $\mu\text{g}$  of Dela) was added; in well-2, an equivalent quantity of Dela-PNP nanosuspension ( $\approx 50$   $\mu\text{g}$  of Dela) was added; and in well-3, the same amount of blank nanoparticles (B-PNPs) was added. After the plates were allowed to stand for 2 h, they were incubated at  $37 \pm 1$  °C for 24 h. The zones of inhibition produced by the different formulations were measured (millimeters) in triplicate.

**2.10. Physical Stability.** The optimal Dela-PNPs were periodically evaluated for storage stability based on size characteristics,  $\zeta$ -potential, drug encapsulation, and loading capacity.<sup>16,33</sup> Precisely weighed samples (10 mg) of freeze-dried Dela-PNPs were placed in glass containers. Over a 6-month period, three containers were stored at  $25 \pm 2$  °C with  $75 \pm 5\%$  relative humidity (RH), while another three were kept at  $37 \pm 2$  °C with  $75 \pm 5\%$  RH. At specified intervals (1 week, 1, 3, and 6 months), the samples were examined for changes in the aforementioned parameters. Before each assessment, the stored samples were reconstituted by being suspended in simulated tear fluid (STF).

**2.11. Statistical Analysis.** All results are expressed as the mean of at least three measurements with standard deviations (mean  $\pm$  SD) unless otherwise indicated. The comparison between the mean values was performed by applying a one-way analysis of variance (ANOVA) using GraphPad Prism

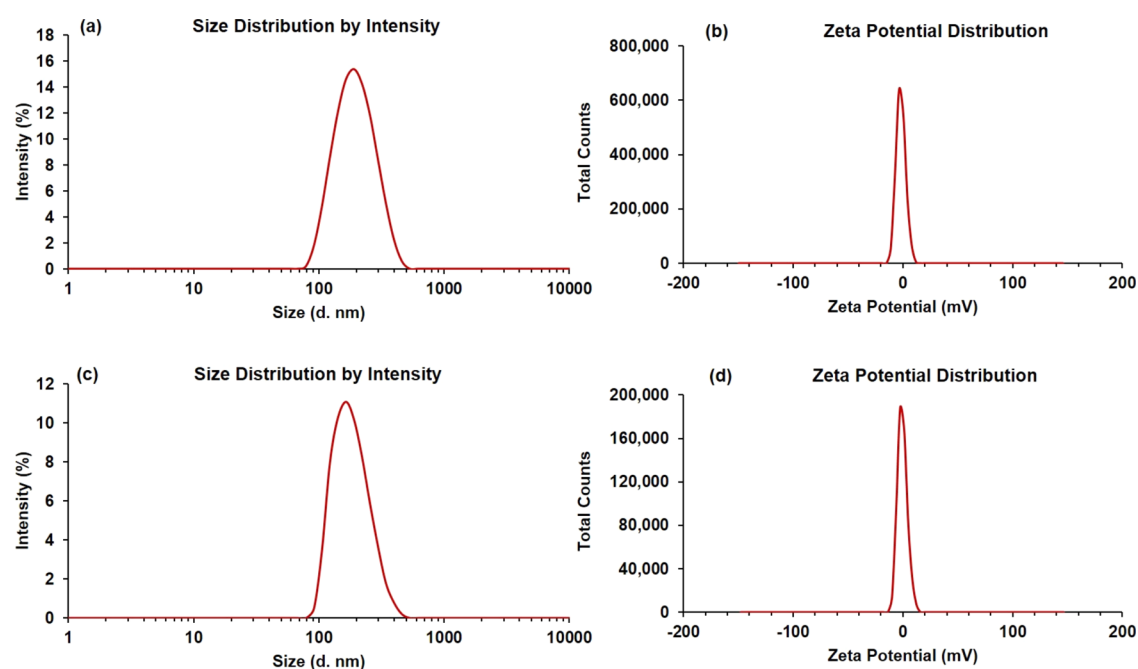
**Table 1. Preparation of Blank PLGA Nanoparticles (B-PNPs) for the Optimization of the Amount of PLGA (mg) and Concentration of the Stabilizer Poly(vinyl alcohol), PVA**

B-PNPs	formulation factors		outcome parameters (mean $\pm$ SD, $n = 3$ )		
	PLGA (mg)	PVA (% w/v)	particle size (nm)	polydispersity index (PDI)	$\zeta$ -potential (mV)
Blank-1	20.0	0.25	246.7 $\pm$ 8.9	0.537 $\pm$ 0.042	1.67 $\pm$ 0.86
Blank-2	20.0	0.5	222.1 $\pm$ 10.2	0.521 $\pm$ 0.041	2.04 $\pm$ 0.97
Blank-3	20.0	1.0	201.2 $\pm$ 9.3	0.469 $\pm$ 0.039	1.76 $\pm$ 0.84
Blank-4	40.0	0.25	244.6 $\pm$ 10.1	0.253 $\pm$ 0.041	2.06 $\pm$ 0.85
Blank-5	40.0	0.5	212.1 $\pm$ 11.6	0.247 $\pm$ 0.038	2.56 $\pm$ 1.01
Blank-6	40.0	1.0	204.6 $\pm$ 9.9	0.246 $\pm$ 0.034	2.34 $\pm$ 0.96
Blank-7	60.0	0.25	260.4 $\pm$ 12.5	0.412 $\pm$ 0.037	1.47 $\pm$ 0.83
Blank-8	60.0	0.5	237.3 $\pm$ 10.6	0.339 $\pm$ 0.042	1.76 $\pm$ 0.84
Blank-9	60.0	1.0	223.6 $\pm$ 9.8	0.326 $\pm$ 0.038	1.68 $\pm$ 0.86

**Table 2. Characteristics of Drug-Loaded PLGA Nanoparticles (Dela-PNPs) Demonstrating the Influence of Formulation Factors on the Properties of the Developed Dela-PNPs<sup>a</sup>**

formulations (Dela-PNPs)	formulation factors		outcome parameters (mean $\pm$ SD, $n = 3$ )				
	Dela (mg)	drug/PLGA (w/w)	particle size (nm)	PDI	$\zeta$ -potential (mV)	%EE	%DL
Batch-1	4.0	1:10	238.9 $\pm$ 10.2	0.258 $\pm$ 0.084	2.78 $\pm$ 0.34	84.6 $\pm$ 7.3	12.9 $\pm$ 1.6
Batch-2	6.0	1.5:10	252.6 $\pm$ 12.2	0.278 $\pm$ 0.045	3.15 $\pm$ 0.62	80.4 $\pm$ 6.1	10.4 $\pm$ 1.8
Batch-3	8.0	2:10	264.5 $\pm$ 13.1	0.303 $\pm$ 0.049	3.05 $\pm$ 0.81	77.4 $\pm$ 5.2	7.7 $\pm$ 1.7

<sup>a</sup>PLGA (40 mg) and stabilizer (PVA, 1%, w/v) were fixed in all three batches.

**Figure 2.** Particle size (a) and  $\zeta$ -potential distributions (b) of Blank PLGA nanoparticles (B-PNPs, Blank-6). Particle size (c) and  $\zeta$ -potential distributions (d) of the optimal Dela-loaded PLGA nanoparticles (Dela-PNPs, Batch-1).

statistical software, followed by “Tukey’s multiple comparison *post hoc* tests”, where  $p < 0.05$  indicates statistical significance.

### 3. RESULTS AND DISCUSSION

**3.1. Formulation Development.** In preliminary trials, a total of nine blank PLGA-based nanoparticles (in triplicate) were prepared by taking varying amounts of PLGA with three concentrations of PVA (%), as shown in Table 1. As the concentrations of PLGA and PVA increased, the nanoparticle size also increased. However, the PDI improved (lowered) at the highest PVA concentration (1%). The  $\zeta$ -potential remained nearly constant across all cases, consistent with

previous observations during the development of lipid–polymer hybrid nanoparticles encapsulated with Dela.<sup>34</sup> Given its smaller size and lower PDI, Blank-6 was selected as the best composition. Therefore, 40 mg of PLGA and PVA (1%) was chosen further to prepare the drug-loaded PLGA nanoparticles (Dela-PNPs), as illustrated in Table 2.

Three different weights of Dela were selected to prepare the drug-loaded PNPs. The formulation using the lowest drug weight (4 mg) with 40 mg of PLGA produced smaller particles (238.9 nm) with a low PDI (0.258) compared to formulations with higher drug amounts using the same PLGA quantity. The  $\zeta$ -potentials of all three formulations were relatively similar.

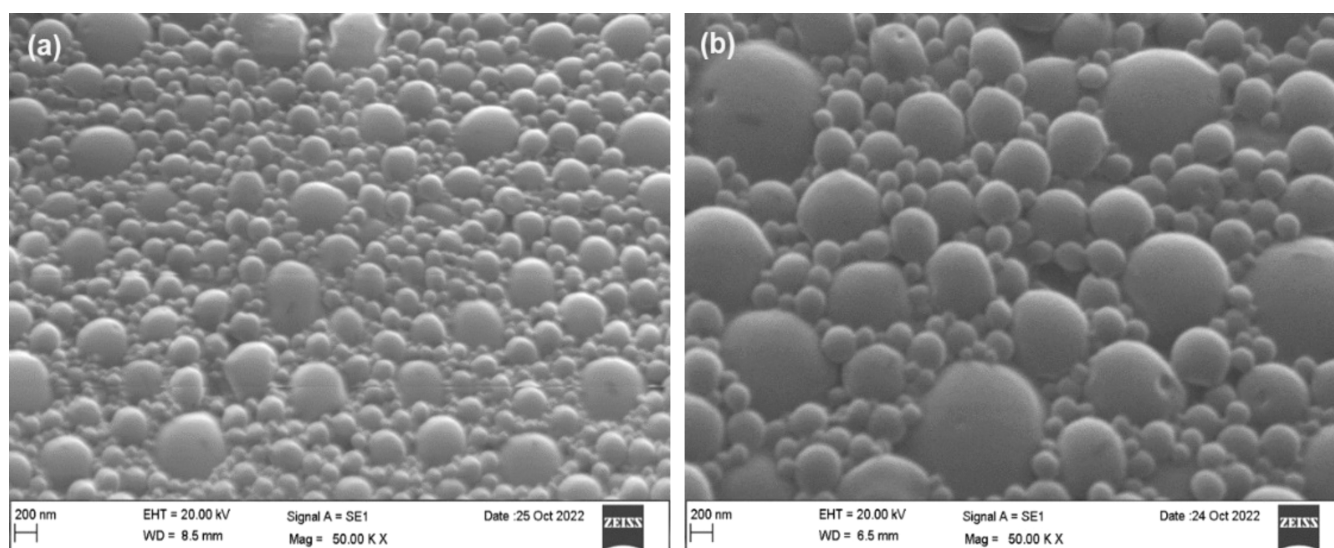


**Figure 3.** Scanning electron microscopy (SEM) images of blank PNPs (a) and Dela-PNPs (b).

However, the encapsulation efficiency (%EE) and drug loading (%DL) were higher for the formulation with a low drug-to-polymer weight ratio (1:10 w/w), achieving approximately 84.6 and 12.9%, respectively (Table 2). The likely reason for this is that the larger surface area of the polymer matrix provided ample space to encapsulate the lipophilic drug (Dela) within the polymer matrix, as suggested by previous reports.<sup>24,35</sup> Additionally, the higher %EE and %DL were likely due to the rapid incorporation of Dela in the core of the nanoparticles, facilitated by the excellent stabilizing capacity of PVA.<sup>13,36</sup> Therefore, Batch-1 (1:10, w/w Dela: PLGA) was chosen as the optimal formulation.

### 3.2. PNP Characterization and Surface Morphology.

The size and  $\zeta$ -potential distributions of the blank PLGA nanoparticles (Blank-6, B-PNPs) and the optimal drug-loaded PLGA nanoparticles (Batch-1, Dela-PNPs) are represented in Figure 2. The average size of B-PNPs prepared using 40 mg of PLGA was  $204.4 \pm 9.9$  nm, while slightly larger particles ( $238.9 \pm 10.2$  nm) were obtained when Dela was loaded.

The size of the drug-loaded PNPs (Batch-2 and Batch-3), as shown in Table 2, was further increased to some extent with an increase in the drug amount. This might be associated with the adsorption of the excess drug on the surface of PNPs, as the extra drug molecules were not entrapped properly into the core of the PNPs. The size range of the drug-loaded nanoparticles (Dela-PNPs) appears suitable for the intended delivery of Dela into the eyes following topical application for the treatment of bacterial eye infections. These size ranges are unlikely to cause eye irritation, as the human eye can tolerate particulate matter up to  $10 \mu\text{m}$ .<sup>37,38</sup> The PDI values were  $0.246 \pm 0.034$  and  $0.258 \pm 0.084$  for B-PNPs and Dela-PNPs, respectively. The low PDI values indicated that the PNPs exhibited a unimodal and narrow size distribution, as illustrated in Figure 2a (for B-PNPs) and Figure 2c (for Dela-PNPs).

Blank (B-PNPs) and drug-loaded optimal (Dela-PNPs) formulations had slightly positive surface charges (Figure 2b for B-PNPs and Figure 2d for Dela-PNPs), and their values were nearly identical (*i.e.*,  $2.34 \pm 0.96$  and  $2.78 \pm 0.34$  mV, respectively). Positively charged particles will interact with the negatively charged mucin layer of eye surfaces, which would prolong the ocular retention of Dela-PNPs, thereby providing

sustained ocular delivery of the loaded drug. The low  $\zeta$ -potential (ZP) values of Blank and Dela-PNPs indicated that the emulsification-solvent evaporation method did not affect the surface charge of the PNPs even in the presence of Dela (anionic fluoroquinolone). It is well-known that the NPs with low ZPs cannot have colloidal stability; thus, the prepared Dela-PNPs should be kept in freeze-dried form rather than aqueous suspension state, which can be reconstituted at the time of its use.<sup>39</sup> According to previous reports, as the pH of PLGA and PVA-based NPs increases, the carbonyl groups in PLGA and  $-\text{OH}$  in PVA get closer to the surface of NPs, resulting in high negative  $\zeta$ -potentials. While at neutral pH, the surface charges of NPs decrease and approach near zero.<sup>40,41</sup> This might be the reason for the low positive  $\zeta$ -potential of Dela-PNPs in this study.

SEM imaging of the B-PNPs and Dela-PNPs showed that they were spherical, solid, dense structures with both smooth and uneven surfaces (Figure 3a,b). The only difference observed was that the freeze-dried Dela-PNPs appeared slightly larger, as shown in Figure 3b. This was also noted when the particle size was measured by the DLS technique.

**3.3. Encapsulation Efficiency (%EE) and Drug-Loading Capacity (%DL).** The %EE and %DL of the optimal Dela-PNPs were comparatively higher than those of the other batches ( $84.6 \pm 7.3$  and  $12.9 \pm 1.7\%$ , respectively). The reasons for the relatively higher %EE and %DL were discussed earlier in the formulation development section. Additionally, the preparation method of Dela-PNPs (emulsification-solvent evaporation) involved dissolving the hydrophobic drug (Dela) and PLGA in acetone (a water-miscible solvent) and then adding this solution drop by drop into an aqueous phase containing a stabilizer (1% PVA) while continuously stirring with a magnetic stirrer. During this process, the droplets solidified and formed PNPs as acetone evaporated. Consequently, the increased %EE and %DL might be attributed to the lipophilicity and strong polarity of delafloxacin due to the presence of a chlorine atom in its molecular structure.<sup>42</sup> Although all three batches of Dela-PNPs were prepared with the same concentration of PVA (1%), some of the outcome parameters (size, %EE, and %DL) varied slightly (Table 2) due to the different amounts of drug used. It is important to note

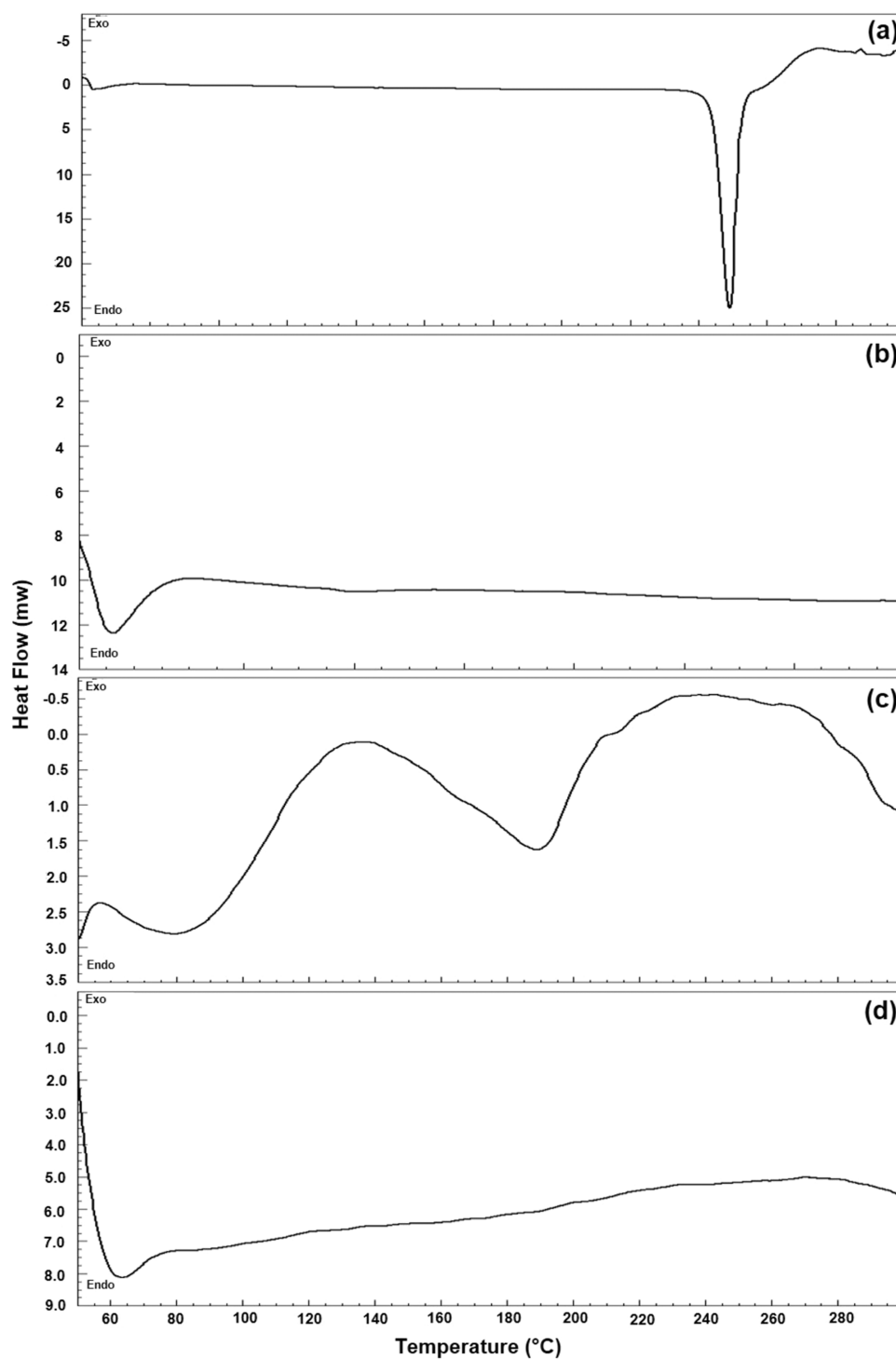


**Figure 4.** Differential scanning calorimetry (DSC) thermograms of pure Dela (a); PLGA (b); a physical mixture (PM) of Dela and PLGA (c); and the freeze-dried Dela-loaded PLGA-based nanoparticles (d).

that using a high amount of Dela to prepare Dela-PNPs by this method is not feasible due to the very low aqueous solubility of Dela during the primary emulsification step.<sup>35</sup>

**3.4. Differential Scanning Calorimetry (DSC).** The thermograms of the pure drug (Dela), polymer (PLGA), physical mixture (PM) of Dela and PLGA, and the freeze-dried drug-loaded polymeric nanoparticles (Dela-PNPs) were obtained by scanning at the temperature range 50–300 °C as represented in Figure 4. The thermogram shows a sharp endothermic peak of pure Dela at 242.54 °C (Figure 4a),

which was close to the reported melting point of Dela and confirmed the crystalline characteristic of the pure drug.<sup>34,43–45</sup> The DSC curve of pure PLGA shows a melting temperature of 62.5 °C without degradation (Figure 4b), which was also reported by de Melo et al.<sup>46</sup>

The PM shows two broad parabolic endotherms; the first one was at around 195.23 °C, which might be due to the evaporation of moisture from the physically admixed PM during heating, suggesting the hygroscopic nature of Dela (Figure 4c). Apart from its hygroscopic nature, Dela has shown

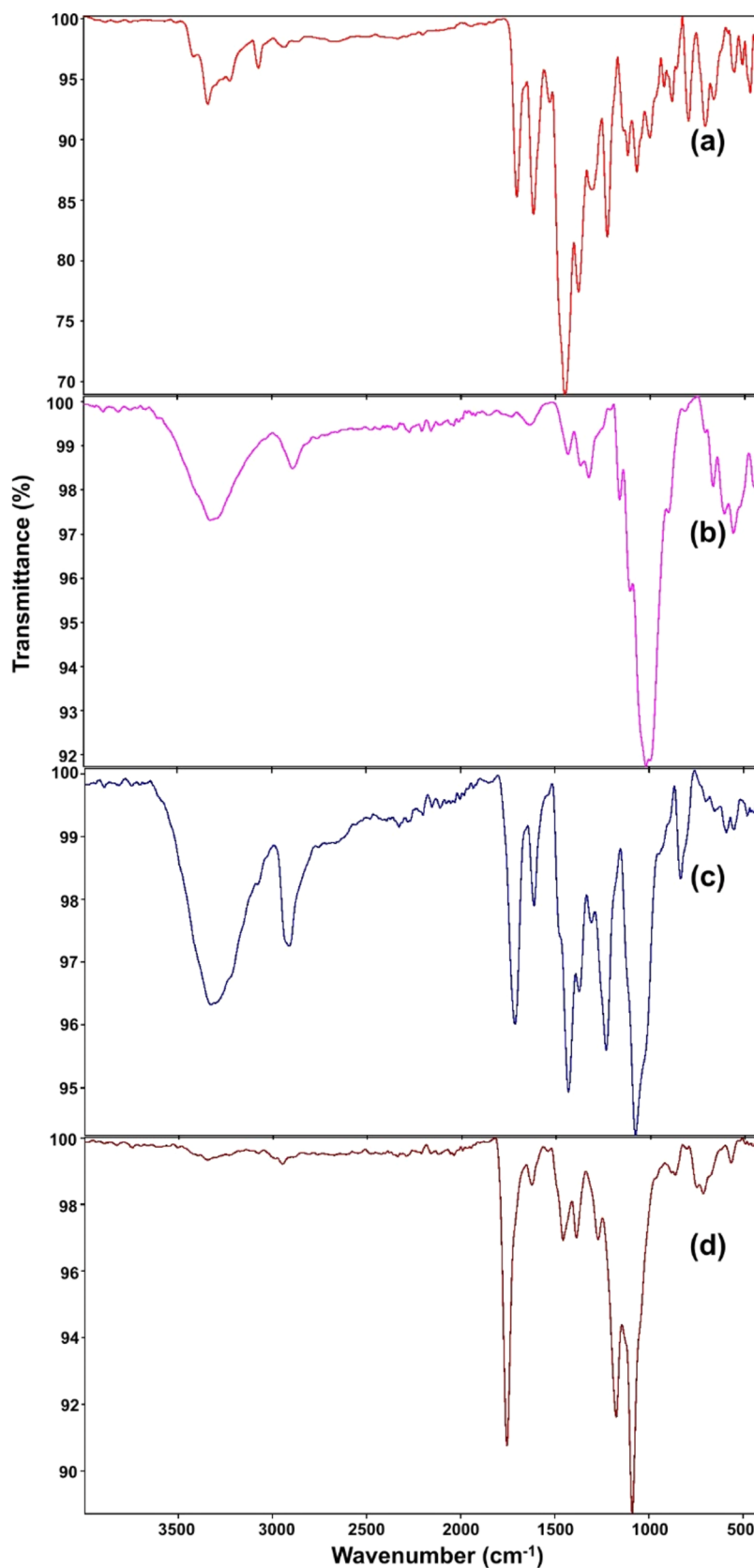


**Figure 5.** FTIR spectra of pure Dela (a); PLGA (b); physical mixture (PM) of Dela and PLGA (c); and freeze-dried Dela-loaded PLGA-based nanoparticles (d).

polymorphism with kinetically stable, metastable, and trihydrate forms.<sup>47</sup> The stable form was variable hemihydrate,

which might be a reason for the slight shift in the melting endotherm of Dela in the PM. The second curve that appeared



around the melting region of PLGA in the same endotherm was associated with the pure PLGA present in the PM. Thus, the endothermic behavior of PLGA and the slightly broad endotherm of melting temperature of Dela was observed in the DSC curve of the PM, indicating the existence of a crystalline state of Dela in the PM.<sup>45</sup> The endotherm associated with Dela did not appear around its melting region in the thermogram of the optimal freeze-dried drug-loaded nanoparticles (Dela-PNPs), as shown in Figure 4d. This clearly demonstrates that the drug was transformed into an amorphous state and encapsulated maximally in the matrix of the PLGA during the preparation of PNPs and the process of freeze-drying completely dried the product. However, a slightly depressed endotherm appeared in the same thermogram around the melting region of PLGA, which might be due to the bulk amount of PLGA in the drug-loaded PNPs.

**3.5. FTIR Analysis.** The FTIR spectra of pure Dela, PLGA, PM of Dela and PLGA, and Dela-PNPs were obtained by FTIR spectroscopy in the wavenumber range of 400–4000  $\text{cm}^{-1}$ , as represented in Figure 5. One of the objectives of performing an FTIR spectral analysis was to check the compatibility of Dela with PLGA while encapsulated into the PNPs in association with the identification, characterization, and purity check of the drug. The characteristic bands of Dela that appeared in the spectra showed strong C=O stretching (conjugated aldehyde or conjugated acid) at wavenumber 1704.4  $\text{cm}^{-1}$ , C=C stretching of  $\alpha$ - $\beta$ -unsaturated ketones at 1616.3  $\text{cm}^{-1}$ , strong N–O stretching (nitro compound) at 1530.5  $\text{cm}^{-1}$ , strong C–F stretching (fluoro compound) at 1452.7  $\text{cm}^{-1}$ , C–H bending (alkane) at 1378.2  $\text{cm}^{-1}$ , strong C–O stretching in association with strong C–N stretching at 1226.3  $\text{cm}^{-1}$ , and strong C–O stretching (primary alcohol) at 1069.8  $\text{cm}^{-1}$  (Figure 5a), which may confirm the purity of Dela.<sup>34,45</sup> The FTIR spectra of PLGA (Figure 5b) have C–H bending vibration bands at 1084.09, 1170.09, and 1268.39  $\text{cm}^{-1}$ . Also, the IR spectra of PLGA have the bending vibration of C=O (at 1385.87  $\text{cm}^{-1}$ ), –COO stretching (at 1747.39  $\text{cm}^{-1}$ ), and C–H stretching vibration (at 2951.87  $\text{cm}^{-1}$ ). These are the characteristic bands of IR spectra of PLGA.<sup>48</sup>

The above-identified IR bands of Dela were obvious and remarkable in the IR spectra of PM, as shown in Figure 5c. Also, the important and characteristic bands of Dela were distinct in the IR spectra of Dela-PNPs, approximately at the same wavenumbers (Figure 5d), and they precisely coincided with the spectra of PM with subtle shifting in their position. This indicates the nonexistence of any covalent interactions between Dela and PLGA, as well as drug and other solvents used during the preparation of PNPs. Some bands of Dela were either missing or appeared with reduced intensity in the IR spectra of Dela-PNPs, which might be due to the overlapping of distinct bands of PLGA and Dela. This was also reported previously during the development of lipid–polymer-based nanoformulation<sup>34</sup> and nanoparticulate solid dispersions<sup>45</sup> of Dela.

**3.6. In Vitro Release of Dela from Dela-PNPs and Release Mechanism.** The release of drug from the pure drug suspension was faster and relatively high during the initial hours (till 12 h) and reached up to  $32.08 \pm 6.36\%$ . The %DR remained nearly unchanged even after 24 h of incubation in the release medium ( $32.72 \pm 6.34\%$ ). After that, a very slow drug release was noted, which was  $34.61 \pm 6.02\%$  at 36 h and reached  $44.56 \pm 5.77\%$  at the end (until 96 h). In contrast, the drug release from PNPs was sustained, and only a small

fraction of the loaded drug was released ( $21.30 \pm 1.39\%$ ) within the first 12 h. After 12 h, the drug release from PNPs was increased linearly (as seen in Figure 6), reaching

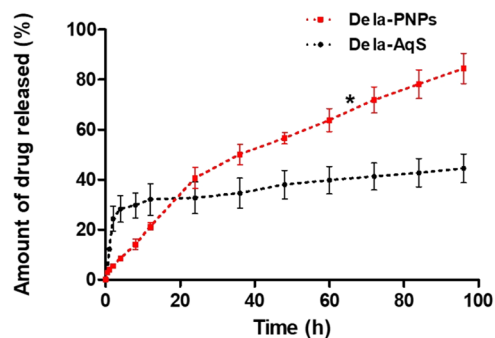


**Figure 6.** *In vitro* release of Dela from Dela-PNPs and control formulation (Del-AqS). Results are the averages of three measurements with standard deviations (mean  $\pm$  SD,  $n = 3$ ). \*  $p < 0.05$ , significantly improved release of the drug occurred from PNPs as compared to AqS.

approximately  $40.64 \pm 4.22\%$  at 24 h and  $50.08 \pm 4.15\%$  at 36 h. The cumulative drug release continued to increase at subsequent time points, ultimately reaching a maximum of  $84.47 \pm 6.11\%$  at 96 h. Therefore, sustained drug release was noted from the Dela-loaded PNPs.

A biphasic release of Dela was found from Dela-PNPs during the *in vitro* release experiment with an initial rapid release ( $40.64 \pm 4.22\%$ ) at 24 h, which might be attributed to the surface-adsorbed drug on the polymeric matrix of PLGA nanoparticles. The surface-adsorbed drug molecules were desorbed rapidly when the PNPs came in contact with the release medium (STF), which was also found during the *in vitro* release of rifampicin from the PLGA-based NPs.<sup>49</sup> The second phase showed a slower/sustained release of the drug as the encapsulated drug was diffused out slowly from the PLGA matrix into the release medium, and around  $84.47 \pm 6.11\%$  of the drug was released within 96 h. The sustained release of drug from Dela-PNPs was at a constant rate, where the concentration of the drug was above the MIC<sub>90</sub> range (0.015 to 2.0  $\mu\text{g}/\text{mL}$  against the Gram-positive pathogens). At this concentration range, among *S. aureus*, approximately 83.6% of MRSA strains were found to be inhibited at the susceptible breakpoint of  $\leq 0.25 \mu\text{g}/\text{mL}$ .<sup>50</sup>

The mechanism of drug release is considered as the rate-limiting step that controls the rate of drug release from a carrier/nanocarrier until the exhaustion of drug release. The diffusion of the encapsulated drug into the polymer matrix, solvent penetration into carriers (responsible for swelling of the carriers), erosion and degradation of the polymeric matrix, or the combination of all of these are the main mechanisms of drug release. The degradation of PLGA occurs by hydrolytic cleavage of the polyester backbone.<sup>51,52</sup> As the degradation of PLGA is a very slow process, the release of Dela from PNPs was associated mainly with the erosion/degradation of PLGA and, to some extent, due to the diffusion of the drug from the PLGA matrix into the medium.<sup>49,51,53,54</sup>

In the present investigation, the mechanism of drug release from Dela-PNPs primarily followed the Higuchi-matrix model, where the value of the correlation coefficient ( $R^2$ ) was highest (0.9936) and the second best-fit was the first-order model ( $R^2 = 0.9935$ ). There was linearity in the release profile of Dela

from PNPs from the PLNs, as summarized in Table 3 and represented well in Figure 7. Considering the highest  $R^2$  values

**Table 3. Kinetic Investigation of the Drug Released from the Delafloxacin-Loaded PLGA Nanoparticles (Del-PNPs)**

applied release models	$R^2$	slope	$^a n$ -values
zero order (fraction of drug released versus time)	0.9593	0.0088	
first order (log% drug remaining versus time)	0.9935	0.0079	0.0034
Korsmeyer–Peppas (log fraction of drug released versus log time)	0.9923	0.6829	
Hixson–Crowell ( $M_0^{1/3} - M_t^{1/3}$ versus time)	0.7405	0.0364	
Higuchi matrix (fraction of drug released versus square root of time)	0.9936	0.0934	0.0407

<sup>a</sup> $n$ -values indicate the values of the release exponent or diffusion exponent.

and using the values of the slope of these plots, the release exponents ( $n$ -values) were calculated and found to be 0.0407 and 0.0034 for the Higuchi-matrix and first-order kinetic models, respectively. The calculation of  $n$ -values suggested that the drug release from PNPs followed the Fickian diffusion mechanism.

Though zero-order release kinetics is considered the most appropriate, where the rate of release is completely independent of the concentration of dissolved drug into the release medium, and the drug is released at a constant rate throughout the time course. However, this type of release kinetics was impractical in the case of PLGA-based nanoparticles. Therefore, erosion/degradation of the PLGA matrix can be the most appropriate mechanism that is of nonzero order type, where the release rate is dependent on the degradation kinetics of PLGA.<sup>51</sup> Also, the drug diffusion mechanism can be the second most prevalent mechanism,

which is dependent on the concentration of dissolved drug as defined by “Fick’s second Law”, where the concentration gradient varies with time length. Based on the drug release pattern and release mechanism, the developed Dela-PNPs can be applied as a single topical dose into the infected eyes, which would maintain the therapeutic level of the drug (which was much more than its MIC<sub>90</sub> value) for a prolonged period of time (24 h) and the Dela-PNPs would be an ideal nanocarrier system for ocular use.

There is a substantial amount of published literature on the mathematical modeling of drug release kinetics from PLGA-based nanoparticles. However, the benefits of this approach have not been adequately emphasized. Therefore, it is important to focus on the application of mechanistic models instead of solely relying on mathematical models. This shift would enhance our understanding of release mechanisms and improve the extrapolation for various polymeric drug delivery systems.<sup>51,54</sup> Therefore, there remains significant potential for developing new modeling approaches to provide better and innovative toolkits, which can help avoid the trial-and-error methods currently used to achieve the desired and predictable outcomes.

**3.7. Sterility Testing and Minimum Inhibitory Concentrations (MICs).** During the incubation period of the optimized formulation in the sterility testing, both media were visually examined every day for 14 days to check the appearance of cloudiness/turbidity due to any microbial growth. In this investigation, no turbidity was observed in both media, confirming the absence of any viable microorganisms. The absence of turbidity for the tested products (even on the 14th day) indicated that these were sterile. Thus, the developed products would be safe and suitable for ophthalmic applications.<sup>55</sup>

The minimum inhibitory concentrations (MICs) of a pure drug (Dela-AqS) and Dela-PNPs against the tested Gram-

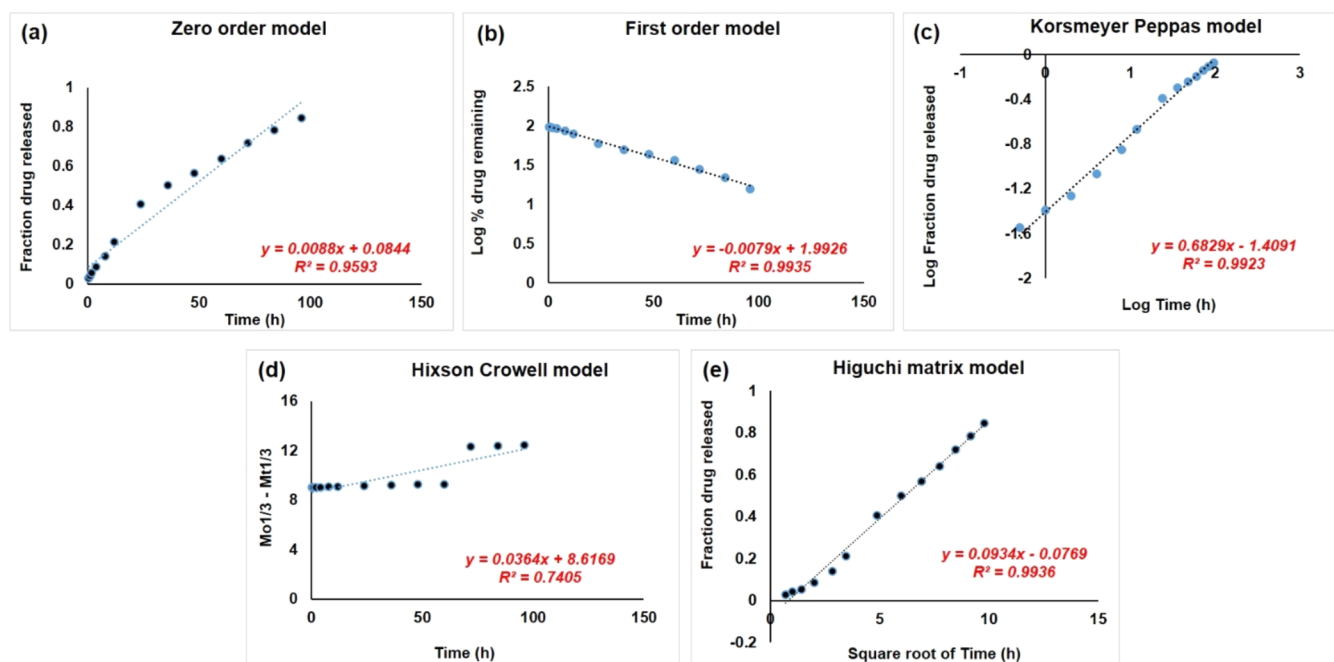


**Figure 7.** Fitting of release data obtained from the *in vitro* drug release profiling of Dela-PNPs in different kinetic models. (a) Zero-order; (b) first-order; (c) Korsmeyer–Peppas; (d) Hixson–Crowell, and (e) Higuchi matrix models. *In vitro* drug release study was performed using STF (pH 7.4) as a release medium accompanied by Tween 80 (0.5%, w/v) at ocular surface temperature ( $35 \pm 1$  °C).

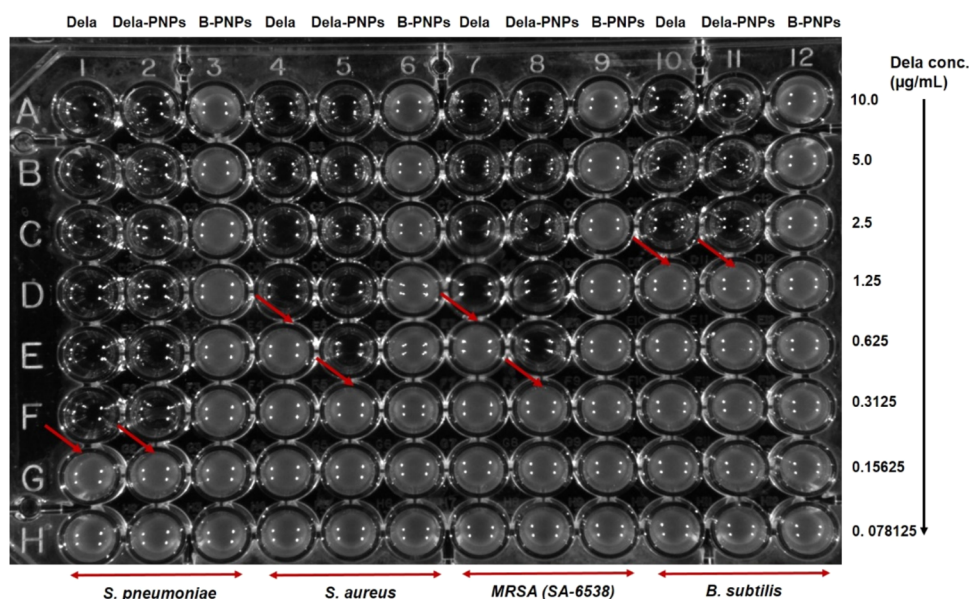


**Figure 8.** MICs of Dela (concentration range of 0.078–10  $\mu\text{g/mL}$ ) in Dela-AqS and Dela-PNPs as compared with B-PNPs against the Gram-positive microbes.

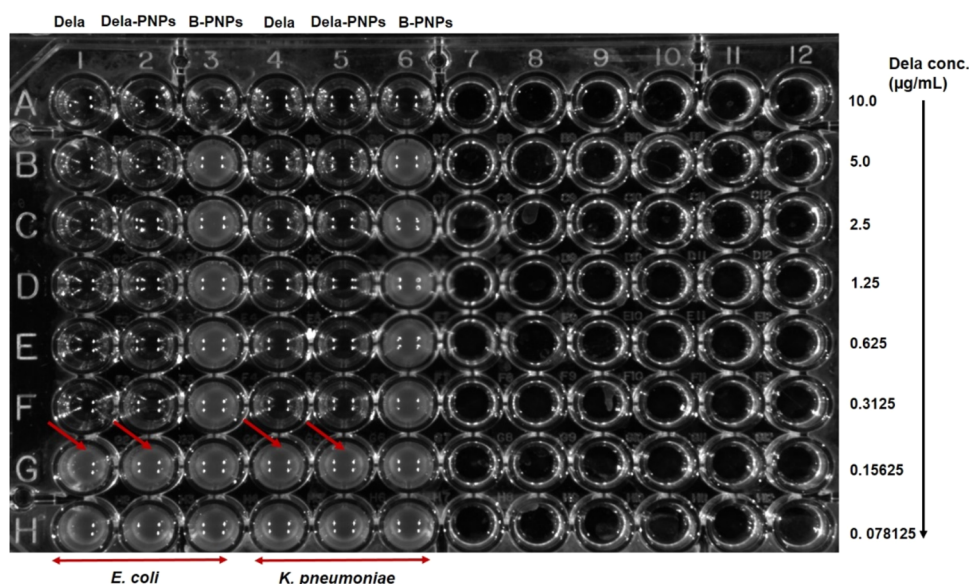


**Figure 9.** MICs of Dela (concentration range of 0.078–10  $\mu\text{g/mL}$ ) in Dela-AqS and Dela-PNPs as compared to B-PNPs against the Gram-negative pathogens.

positive and Gram-negative pathogens were determined using optical density measurements. This was needed to evaluate the enhanced antimicrobial activity of Dela while being loaded in PNPs. The results indicate that in the presence of blank nanoparticles (B-PNPs, control experiments), the optical density associated with microbial growth increased. However, as the concentration of Dela-containing formulations increased, the optical density of the microorganisms decreased, aligning with previous reports on Dela.<sup>4,56,57</sup> The MICs of Dela were measured in a concentration range of 0.078–10  $\mu\text{g/mL}$ . The determined MICs of Dela in Dela-AqS and Dela-PNPs, compared to B-PNPs, against the Gram-positive (Figure 8) and Gram-negative (Figure 9) pathogens are summarized in Table 4. The results indicated a higher susceptibility of *S. pneumoniae*, *K. pneumoniae*, and *E. coli* at the lowest

**Table 4. Minimum Inhibitory Concentration (MICs) Values of Dela from Dela-AqS and Dela-PNPs against Some Gram-Positive and Gram-Negative Microorganisms**

microorganisms	MICs of dela present in different formulations		
	Dela-AqS	Dela-PNPs	B-PNPs
Gram-Positive			
<i>S. pneumoniae</i>	0.3125 $\mu\text{g/mL}$	0.3125 $\mu\text{g/mL}$	not obtained
<i>S. aureus</i>	1.25 $\mu\text{g/mL}$	0.63 $\mu\text{g/mL}$	not obtained
MRSA (SA-6538)	1.25 $\mu\text{g/mL}$	0.63 $\mu\text{g/mL}$	not obtained
<i>B. subtilis</i>	2.50 $\mu\text{g/mL}$	2.50 $\mu\text{g/mL}$	not obtained
Gram-Negative			
<i>E. coli</i>	0.3125 $\mu\text{g/mL}$	0.3125 $\mu\text{g/mL}$	not obtained
<i>K. pneumoniae</i>	0.3125 $\mu\text{g/mL}$	0.3125 $\mu\text{g/mL}$	not obtained

Table 5. Antimicrobial Activity of Dela-Containing Products<sup>a,b</sup>

		(a) antimicrobial vulnerability of Dela containing products			
		zone of inhibitions (mm), mean $\pm$ SD, $n = 3$			
microorganisms		Dela-AqS	Dela-PNPs	B-PNPs	fold increased (PNPs/AqS)
Gram-positive	<i>S. pneumoniae</i>	27.4 $\pm$ 1.6	37.0 $\pm$ 3.2	8.2 $\pm$ 0.8	1.35
	<i>S. aureus</i>	24.3 $\pm$ 1.7	34.6 $\pm$ 2.4	6.7 $\pm$ 0.2	1.42
	MRSA (SA-6538)	23.7 $\pm$ 1.5	34.8 $\pm$ 2.2	7.4 $\pm$ 0.2	1.46
	<i>B. subtilis</i>	22.4 $\pm$ 1.6	31.2 $\pm$ 2.3	7.0 $\pm$ 0.7	1.38
Gram-negative	<i>K. pneumoniae</i>	27.5 $\pm$ 1.2	35.9 $\pm$ 2.6	7.6 $\pm$ 0.6	1.31
	<i>E. coli</i>	28.2 $\pm$ 1.4	35.9 $\pm$ 1.1	8.3 $\pm$ 0.7	1.28

(b) significance level by one-way ANOVA followed by "Tukey's multiple comparison test"				
comparison test	mean difference	$q (\sqrt{2*D/SED})$	significance level ( $p < 0.05$ )	95% CI of difference
Dela-AqS vs Dela-PNPs	-8.867	10.30	yes (***)	-12.03 to -5.703
Dela-AqS vs B-PNPs	18.53	21.53	yes (***)	15.37 to 21.70
Dela-PNPs vs B-PNPs	27.40	31.82	yes (***)	

<sup>a</sup>Data analysis with one-way analysis of variance <sup>b</sup>Where "D" is the difference between the two means, SED is the standard error of that difference, and CI is the confidence interval.

concentration ( $\sim 0.31 \mu\text{g/mL}$ ) toward Dela as compared to other microorganisms in the present investigation.

Similarly, the susceptibility of *S. aureus* and MRSA-6538 strains in the case of Dela-PNPs was higher ( $\sim 0.63 \mu\text{g/mL}$ ) compared to that of *B. subtilis* ( $2.5 \mu\text{g/mL}$ ). This finding was in agreement with previous reports where the methicillin-sensitive *S. aureus* (MSSA) and MRSA were found to be  $\sim 98$  and  $\sim 87\%$  susceptible, respectively, to Dela after 24 h incubation.<sup>2,58</sup>

The obtained MICs were equivalent to the reported values of an aromatically fused imidazole derivative (structurally similar to Dela), where the antibacterial activity against MRSA was noted at  $512 \mu\text{g/mL}$  of MICs.<sup>59,60</sup> This compound also showed strong activity against *K. pneumoniae* with MICs of  $0.5 \mu\text{g/mL}$ , *E. coli* with MICs of  $0.25 \mu\text{g/mL}$ , *P. aeruginosa* with MICs of  $1 \mu\text{g/mL}$ , and *Acinetobacter baumannii* with MICs of  $0.5 \mu\text{g/mL}$ .<sup>60,61</sup>

**3.8. Antibacterial Activity of Dela-PNPs.** The results of the antimicrobial activity of Dela-containing products against the chosen microorganisms are summarized in Table 5. The Dela-PNPs, as compared to Dela-AqS, showed a significant improvement ( $p < 0.05$ ) in the antimicrobial potency of Dela against the used bacterial strains. The blanks (B-PNPs) did not show any inhibitory effect on bacterial growth (Figure 10).

From the previous reports, it was found that Dela is a broad-spectrum antibiotic with prolonged antibacterial activity against Gram-positive microorganisms, including the quinolone-resistant *S. pneumoniae* and *S. aureus*. Dela has an antibacterial activity comparable to that of ciprofloxacin (MIC  $0.06\text{--}0.25 \mu\text{g/mL}$ ) against *P. aeruginosa*. It has shown a notable *in vitro* activity against *Mycobacterium tuberculosis*, *Helicobacter pylori*, and *Mycoplasma pneumoniae* with MIC values of  $0.25\text{--}8 \mu\text{g/mL}$ .<sup>62-64</sup>

With the blanks (B-PNPs), virtually no antibacterial activity was detected. The results are summarized in Table 5b. The amplified activity of Dela-PNPs compared to Dela-AqS indicated that the process variables and steps could not adversely affect the primary structural activity relationship and basic antibacterial potency of Dela. Eventually, the loading of Dela into PLGA nanoparticles (PNPs) would not only maintain its antibacterial potency but also be expected to improve its bioavailability for the treatment of bacterial infections in the eyes.

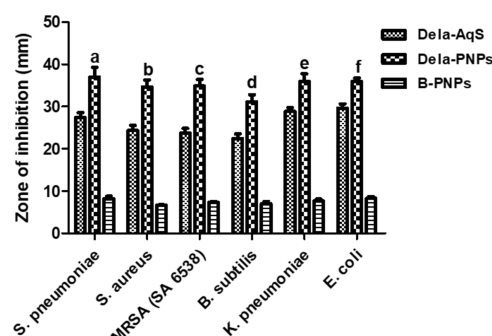


**Figure 10.** Antimicrobial activity of Dela-PNPs and Dela-AqS as compared to B-PNPs against *S. pneumoniae*, *S. aureus*, MRSA (SA-6538), *B. subtilis*, *K. pneumoniae*, and *E. coli*. Results include average and standard deviations of triplicate measurements of inhibition zones. Where "a"  $p < 0.05$ , Dela-PNPs versus Dela-AqS (for *S. pneumoniae*); "b"  $p < 0.05$ , Dela-PNPs versus Dela-AqS (for *S. aureus*); "c"  $p < 0.05$ , Dela-PNPs versus Dela-AqS (for MRSA: SA-6538); and "d"  $p < 0.05$ , Dela-PNPs versus Dela-AqS (for *B. subtilis*). Similarly, "e"  $p < 0.05$ , Dela-PNPs versus Dela-AqS (for *K. pneumoniae*) and "f"  $p < 0.05$ , Dela-PNPs versus Dela-AqS (for *E. coli*).

**3.9. Stability Study.** The optimal formulation (Dela-PNPs) was evaluated periodically to evaluate its physical stability. This study was performed to establish the limits of stability for the maintenance of its storage at ambient ( $25 \pm 2 \text{ }^\circ\text{C}$ ) and slightly elevated ( $37 \pm 2 \text{ }^\circ\text{C}$ ) temperatures for a period of 6 months. The outcomes of the evaluated parameters are detailed in Table 6.

The stability results did not indicate any remarkable change in the PDI and  $\zeta$ -potential of the stored sample under both storage conditions. A slight increase in the particle size was noted at  $25 \text{ }^\circ\text{C}$  while it was a little higher at the stressed temperature ( $37 \text{ }^\circ\text{C}$ ). A subtle increase in the particle sizes was noted at 6 months of storage at  $25 \pm 2 \text{ }^\circ\text{C}$  ( $\pm 10 \text{ nm}$ ) and  $37 \pm 2 \text{ }^\circ\text{C}$  ( $\pm 17 \text{ nm}$ ). A related but nonsignificant size increase of PLGA-based NPs has also been reported at the same storage conditions.<sup>13,65</sup>

No alteration in %DL was noted throughout the storage period. However, a minor reduction in the %EE was found at both temperatures on prolonged storage, especially in the third and 6 months. A significant increase in the size of the freeze-dried PNPs in the present investigation was obtained at  $37 \text{ }^\circ\text{C}$ ,

**Table 6. Effect on the Selected Outcome Parameters of Dela-PNPs for 6 Months of Storage at  $25 \pm 2$  and  $37 \pm 2$  °C Temperature Conditions<sup>a</sup>**

time points	evaluated parameters (mean $\pm$ SD, $n = 3$ )				
	particle size (nm)	PDI	$\zeta$ -potential (mV)	%EE	%DL
Stored at $25 \pm 2$ °C					
initially (0 h)	238.9 $\pm$ 10.2	0.258 $\pm$ 0.084	2.78 $\pm$ 0.34	84.6 $\pm$ 7.2	7.6 $\pm$ 0.6
at 1 week	241.4 $\pm$ 8.8	0.262 $\pm$ 0.085	2.76 $\pm$ 0.32	83.1 $\pm$ 8.4	7.5 $\pm$ 0.8
at 1 month	244.4 $\pm$ 6.7	0.272 $\pm$ 0.078	2.73 $\pm$ 0.34	81.9 $\pm$ 9.1	7.4 $\pm$ 0.8
at 3 months	248.2 $\pm$ 10.7	0.282 $\pm$ 0.088	2.68 $\pm$ 0.31	79.8 $\pm$ 10.8	7.3 $\pm$ 0.9
at 6 months	249.8 $\pm$ 8.2	0.302 $\pm$ 0.097	2.64 $\pm$ 0.44	77.9 $\pm$ 11.3	7.0 $\pm$ 1.0
Stored at $37 \pm 2$ °C					
initially (0 h)	238.9 $\pm$ 10.2	0.258 $\pm$ 0.083	2.78 $\pm$ 0.33	84.5 $\pm$ 7.3	7.6 $\pm$ 0.6
at 1 week	243.8 $\pm$ 9.4	0.267 $\pm$ 0.084	2.74 $\pm$ 0.31	82.6 $\pm$ 8.5	7.6 $\pm$ 0.8
at 1 months	247.1 $\pm$ 9.0	0.278 $\pm$ 0.086	2.78 $\pm$ 0.32	80.8 $\pm$ 10.4	7.4 $\pm$ 0.9
at 3 months	252.4 $\pm$ 11.6	0.288 $\pm$ 0.091	2.63 $\pm$ 0.31	78.1 $\pm$ 13.9	7.1 $\pm$ 1.3
at 6 months	255.2 $\pm$ 8.4	0.312 $\pm$ 0.089	2.54 $\pm$ 0.31	76.3 $\pm$ 13.4	6.9 $\pm$ 1.2

<sup>a</sup>The data were represented as the mean of three measurements with standard deviations (mean  $\pm$  SD,  $n = 3$ ).

which was attributed to dehydration of the stabilizer (PVA), which might have prevented the protection of the particles and resulted in minor aggregation. Another possibility is that there might be a minor hydrolytic degradation of PLGA at elevated temperatures.<sup>66</sup> At the same time, loss by degradation of the entrapped drug may occur, which could lead to a decrease in the %EE.<sup>67</sup> Taken together, Dela-PNPs were more stable upon storage at 25 °C without any significant size increase or loss of encapsulated drug for up to 6 months.

#### 4. CONCLUSIONS

Dela was successfully encapsulated into PNPs by the double emulsion-solvent-evaporation method. The developed formulation was spherical, optimally sized, uniformly distributed, and slightly positively charged with Dela-PNPs. Dela-PNPs demonstrated a significantly higher antimicrobial activity compared with an aqueous suspension (Dela-AqS) against several Gram-positive and Gram-negative bacteria. Moreover, the developed Dela-PNPs were found to be stable at 25 and 37 °C for 6 months. Therefore, we conclude that encapsulation of Dela into PLGA nanoparticles would be a promising delivery carrier for ocular applications. Additional experiments, such as *in vivo* eye irritation, ocular pharmacokinetics, and pharmacodynamics in animal models, are needed to confirm the safety, bioavailability, and efficacy of Dela-loaded PLGA nanoparticles.

#### ■ ASSOCIATED CONTENT

##### Data Availability Statement

The data used is available throughout the manuscript text.

#### ■ AUTHOR INFORMATION

##### Corresponding Author

**Aliyah A. Almomen** – Department of Pharmaceutical Chemistry, College of Pharmacy, King Saud University, Riyadh 11491, Saudi Arabia; Email: [alalmomen@ksu.edu.sa](mailto:alalmomen@ksu.edu.sa)

##### Authors

**Abdullah K. Alshememry** – Department of Pharmaceutics, College of Pharmacy, King Saud University, Riyadh 11451, Saudi Arabia; [orcid.org/0000-0002-1306-1625](https://orcid.org/0000-0002-1306-1625)

**Mohd Abul Kalam** – Department of Pharmaceutics, College of Pharmacy, King Saud University, Riyadh 11451, Saudi Arabia; [orcid.org/0000-0002-5713-8858](https://orcid.org/0000-0002-5713-8858)

**Mudassar Shahid** – Department of Pharmaceutics, College of Pharmacy, King Saud University, Riyadh 11451, Saudi Arabia

**Raisuddin Ali** – Department of Pharmaceutics, College of Pharmacy, King Saud University, Riyadh 11451, Saudi Arabia; [orcid.org/0000-0001-9892-2158](https://orcid.org/0000-0001-9892-2158)

**Sulaiman S. Alhudaithi** – Department of Pharmaceutics, College of Pharmacy, King Saud University, Riyadh 11451, Saudi Arabia

**Nada A. Alshumaimeri** – Al-Ghad International Colleges for Applied Medical Sciences, Riyadh 13629, Saudi Arabia

**Ziyad A. BinHudhud** – Department of Pharmaceutics, College of Pharmacy, King Saud University, Riyadh 11451, Saudi Arabia

**Abdulrazzaq A. Aldaham** – Department of Pharmaceutics, College of Pharmacy, King Saud University, Riyadh 11451, Saudi Arabia

**Ziyad Binkhathlan** – Department of Pharmaceutics, College of Pharmacy, King Saud University, Riyadh 11451, Saudi Arabia; [orcid.org/0000-0003-1853-7490](https://orcid.org/0000-0003-1853-7490)

Complete contact information is available at:

<https://pubs.acs.org/10.1021/acsomega.4c07805>

#### Funding

The authors extend their appreciation to the Deputyship for Research and Innovation, Ministry of Education in Saudi Arabia, for funding this research work through project number (DRI-KSU-863).

#### Notes

The authors declare no competing financial interest.

The graphical abstract was created with BioRender <https://biorender.com/>.

#### ■ REFERENCES

- (1) Hori, T.; Owusu, Y. B.; Sun, D. US FDA-Approved Antibiotics During the 21st Century. In *Encyclopedia of Infection and Immunity*; Rezaei, N., Ed.; Elsevier: Oxford, 2022; pp 556–585.
- (2) Hurst, A. L.; Neemann, K. A.; Chatterjee, A. New Antibiotics. In *Viral, Parasitic, Bacterial, and Fungal Infections*; Bagchi, D.; Das, A.; Downs, B. W., Eds.; Academic Press, 2023; Chapter 55, pp 675–698.

- (3) Hatoum, H. T.; Akhras, K. S.; Lin, S.-J. The attributable clinical and economic burden of skin and skin structure infections in hospitalized patients: a matched cohort study. *Diagn. Microbiol. Infect. Dis.* **2009**, *64* (3), 305–310.
- (4) Lemaire, S.; Tulkens, P. M.; Van Bambeke, F. Contrasting effects of acidic pH on the extracellular and intracellular activities of the anti-gram-positive fluoroquinolones moxifloxacin and delafloxacin against *Staphylococcus aureus*. *Antimicrob. Agents Chemother.* **2011**, *55* (2), 649–658.
- (5) Scott, L. J. Delafloxacin: A Review in Acute Bacterial Skin and Skin Structure Infections. *Drugs* **2020**, *80* (12), 1247–1258.
- (6) Mogle, B. T.; Steele, J. M.; Thomas, S. J.; Bohan, K. H.; Kufel, W. D. Clinical review of delafloxacin: a novel anionic fluoroquinolone. *J. Antimicrob. Chemother.* **2018**, *73* (6), 1439–1451.
- (7) Zafar, A.; Alsaidan, O. A.; Imam, S. S.; Yasir, M.; Alharbi, K. S.; Khalid, M. Formulation and Evaluation of Moxifloxacin Loaded Bilosomes In-Situ Gel: Optimization to Antibacterial Evaluation. *Gels* **2022**, *8* (7), No. 418, DOI: 10.3390/gels8070418.
- (8) Ameerduzzafar; Khan, N.; Alruwaili, N. K.; Bukhari, S. N. A.; Alsuwat, B.; Afzal, M.; Akhter, S.; Yasir, M.; Elmowafy, M.; Shalaby, K.; Ali, A. Improvement of Ocular Efficacy of Levofloxacin by Bioadhesive Chitosan Coated PLGA Nanoparticles: Box-behnken Design, In-vitro Characterization, Antibacterial Evaluation and Scintigraphy Study. *Iran J. Pharm. Res.* **2020**, *19* (1), 292–311.
- (9) Cho, J. C.; Crotty, M. P.; White, B. P.; Worley, M. V. What is old is new again: delafloxacin, a modern fluoroquinolone. *Pharmacother.: J. Human Pharmacol. Drug Ther.* **2018**, *38* (1), 108–121.
- (10) Markham, A. Delafloxacin: first global approval. *Drugs* **2017**, *77*, 1481–1486.
- (11) Shiu, J.; Ting, G.; Kiang, T. K. Clinical pharmacokinetics and pharmacodynamics of delafloxacin. *Eur. J. Drug Metab. Pharmacokinet.* **2019**, *44*, 305–317.
- (12) Hoover, R.; Hunt, T.; Benedict, M.; Paulson, S. K.; Lawrence, L.; Cammarata, S.; Sun, E. Safety, Tolerability, and Pharmacokinetic Properties of Intravenous Delafloxacin After Single and Multiple Doses in Healthy Volunteers. *Clin. Ther.* **2016**, *38* (1), 53–65.
- (13) Kalam, M. A.; Alshamsan, A. Poly (d, l-lactide-co-glycolide) nanoparticles for sustained release of tacrolimus in rabbit eyes. *Biomed. Pharmacother.* **2017**, *94*, 402–411.
- (14) Knop, E.; Knop, N. Anatomy and immunology of the ocular surface. *Chem. Immunol. Allergy* **2007**, *92*, 36–49.
- (15) Zhang, W.; Prausnitz, M. R.; Edwards, A. Model of transient drug diffusion across cornea. *J. Controlled Release* **2004**, *99* (2), 241–258.
- (16) Kalam, M. A. Development of chitosan nanoparticles coated with hyaluronic acid for topical ocular delivery of dexamethasone. *Int. J. Biol. Macromol.* **2016**, *89*, 127–136.
- (17) Kalam, M. A. The potential application of hyaluronic acid coated chitosan nanoparticles in ocular delivery of dexamethasone. *Int. J. Biol. Macromol.* **2016**, *89*, 559–568.
- (18) Alsaidan, O. A.; Zafar, A.; Yasir, M.; Alzarea, S. I.; Alqinyah, M.; Khalid, M. Development of Ciprofloxacin-Loaded Bilosomes In-Situ Gel for Ocular Delivery: Optimization, In-Vitro Characterization, Ex-Vivo Permeation, and Antimicrobial Study. *Gels* **2022**, *8* (11), No. 687, DOI: 10.3390/gels8110687.
- (19) Souza, J. G.; Dias, K.; Pereira, T. A.; Bernardi, D. S.; Lopez, R. F. Topical delivery of ocular therapeutics: carrier systems and physical methods. *J. Pharm. Pharmacol.* **2014**, *66* (4), 507–530.
- (20) Kalam, M. A.; Sultana, Y.; Ali, A.; Aqil, M.; Mishra, A. K.; Chuttani, K.; Aljuffali, I. A.; Alshamsan, A. Part II: Enhancement of transcorneal delivery of gatifloxacin by solid lipid nanoparticles in comparison to commercial aqueous eye drops. *J. Biomed. Mater. Res. A* **2013**, *101A* (6), 1828–1836.
- (21) Joshi, P. H.; Youssef, A. A. A.; Ghonge, M.; Varner, C.; Tripathi, S.; Dudhipala, N.; Majumdar, S. Gatifloxacin Loaded Nano Lipid Carriers for the Management of Bacterial Conjunctivitis. *Antibiotics* **2023**, *12* (8), No. 1316, DOI: 10.3390/antibiot-ics12081318.
- (22) Alkholief, M.; Kalam, M. A.; Alshememry, A. K.; Ali, R.; Alhudaithi, S. S.; Alsaleh, N. B.; Raish, M.; Alshamsan, A. Topical Application of Linezolid-Loaded Chitosan Nanoparticles for the Treatment of Eye Infections. *Nanomaterials* **2023**, *13* (4), No. 681, DOI: 10.3390/nano13040681.
- (23) Vasconcelos, A.; Vega, E.; Perez, Y.; Gomara, M. J.; Garcia, M. L.; Haro, I. Conjugation of cell-penetrating peptides with poly(lactico-glycolic acid)-polyethylene glycol nanoparticles improves ocular drug delivery. *Int. J. Nanomed.* **2015**, *10*, 609–631.
- (24) Shin, S. B.; Cho, H. Y.; Kim, D. D.; Choi, H. G.; Lee, Y. B. Preparation and evaluation of tacrolimus-loaded nanoparticles for lymphatic delivery. *Eur. J. Pharm. Biopharm.* **2010**, *74* (2), 164–171.
- (25) Fujita, E.; Teramura, Y.; Shiraga, T.; Yoshioka, S.; Iwatsubo, T.; Kawamura, A.; Kamimura, H. Pharmacokinetics and tissue distribution of tacrolimus (FK506) after a single or repeated ocular instillation in rabbits. *J. Ocul. Pharmacol. Ther.* **2008**, *24* (3), 309–319.
- (26) Hernandis, V.; Escudero, E.; Marin, P. A novel liquid chromatography-fluorescence method for the determination of delafloxacin in human plasma. *J. Sep. Sci.* **2022**, *45* (3), 706–716.
- (27) SIELC Technologies. HPLC Method for Determination of Delafloxacin on Primesep 100 Column. 2022.
- (28) Ritger, P. L.; Peppas, N. A. A simple equation for description of solute release II. Fickian and anomalous release from swellable devices. *J. Controlled Release* **1987**, *5* (1), 37–42.
- (29) Kupiec, T. C. United States Pharmacopeia Chapter <71> Sterility Tests. *Int. J. Pharm. Compd.* **2007**, *11* (5), 400–403.
- (30) Alshememry, A.; Alkholief, M.; Kalam, M. A.; Raish, M.; Ali, R.; Alhudaithi, S. S.; Iqbal, M.; Alshamsan, A. Perspectives of Positively Charged Nanocrystals of Tedizolid Phosphate as a Topical Ocular Application in Rabbits. *Molecules* **2022**, *27* (14), 4619.
- (31) Ilieva, Y.; Dimitrova, L.; Zaharieva, M. M.; Kaleva, M.; Alov, P.; Tsakovska, I.; Pencheva, T.; Pencheva-El Tibi, I.; Najdenski, H.; Pajeva, I. Cytotoxicity and Microbicidal Activity of Commonly Used Organic Solvents: A Comparative Study and Application to a Standardized Extract from *Vaccinium macrocarpon*. *Toxics* **2021**, *9* (5), No. 92, DOI: 10.3390/toxics9050092.
- (32) Al-Yousef, H. M.; Amina, M.; Alqahtani, A. S.; Alqahtani, M. S.; Malik, A.; Hatshan, M. R.; Siddiqui, M. R. H.; Khan, M.; Shaik, M. R.; Ola, M. S.; Syed, R. Pollen bee aqueous extract-based synthesis of silver nanoparticles and evaluation of their anti-cancer and anti-bacterial activities. *Processes* **2020**, *8* (5), No. 524.
- (33) Tsai, M.-L.; Chen, R.-H.; Bai, S.-W.; Chen, W.-Y. The storage stability of chitosan/tripolyphosphate nanoparticles in a phosphate buffer. *Carbohydr. Polym.* **2011**, *84* (2), 756–761.
- (34) Anwer, M. K.; Iqbal, M.; Muharram, M. M.; Mohammad, M.; Ezzeldin, E.; Aldawsari, M. F.; Alalawi, A.; Imam, F. Development of Lipomer Nanoparticles for the Enhancement of Drug Release, Antimicrobial Activity and Bioavailability of Delafloxacin. *Pharmaceutics* **2020**, *12* (3), No. 252, DOI: 10.3390/pharmaceutics12030252.
- (35) Alshamsan, A. Nanoprecipitation is more efficient than emulsion solvent evaporation method to encapsulate curcubitacin I in PLGA nanoparticles. *Saudi Pharm. J.* **2014**, *22* (3), 219–222.
- (36) Alshamsan, A.; Binkhathlan, Z.; Kalam, M. A.; Qamar, W.; Kfoury, H.; Alghonaim, M.; Lavasanifar, A. Mitigation of Tacrolimus-Associated Nephrotoxicity by PLGA Nanoparticulate Delivery Following Multiple Dosing to Mice while Maintaining its Immunosuppressive Activity. *Sci. Rep.* **2020**, *10* (1), No. 6675.
- (37) Zimmer, A.; Kreuter, J. Microspheres and nanoparticles used in ocular delivery systems. *Adv. Drug Delivery Rev.* **1995**, *16* (1), 61–73.
- (38) Zimmer, A. K.; Zerbe, H.; Kreuter, J. Evaluation of pilocarpine-loaded albumin particles as drug delivery systems for controlled delivery in the eye I. In vitro and in vivo characterisation. *J. Controlled Release* **1994**, *32* (1), 57–70.
- (39) do Reis, S. R. R.; Helal-Neto, E.; da Silva de Barros, A. O.; Pinto, S. R.; Portilho, F. L.; de Oliveira Siqueira, L. B.; Alencar, L. M. R.; Dahoumane, S. A.; Alexis, F.; Ricci-Junior, E.; Santos-Oliveira, R. Dual Encapsulated Dacarbazine and Zinc Phthalocyanine Polymeric

Nanoparticle for Photodynamic Therapy of Melanoma. *Pharm. Res.* **2021**, *38* (2), 335–346.

(40) dos Santos Matos, A. P.; Lopes, D.; Peixoto, M. L. H.; da Silva Cardoso, V.; Vermelho, A. B.; Santos-Oliveira, R.; Vicoso, A. L.; Holandino, C.; Ricci-Junior, E. Development, characterization, and anti-leishmanial activity of topical amphotericin B nanoemulsions. *Drug Delivery Transl. Res.* **2020**, *10* (6), 1552–1570.

(41) Ekinici, M.; Yegen, G.; Aksu, B.; Ilem-Ozdemir, D. Preparation and Evaluation of Poly(lactic acid)/Poly(vinyl alcohol) Nanoparticles Using the Quality by Design Approach. *ACS Omega* **2022**, *7* (38), 33793–33807.

(42) Gulyás, D.; Kamotsay, K.; Szabo, D.; Kocsis, B. Investigation of Delafloxacin Resistance in Multidrug-Resistant *Escherichia coli* Strains and the Detection of *E. coli* ST43 International High-Risk Clone. *Microorganisms* **2023**, *11* (6), No. 1602, DOI: [10.3390/microorganisms11061602](https://doi.org/10.3390/microorganisms11061602).

(43) Anwer, M. K.; Mohammad, M.; Khalil, N. Y.; Imam, F.; Ansari, M. J.; Aldawsari, M. F.; Shakeel, F.; Iqbal, M. Solubility, thermodynamics and molecular interaction studies of delafloxacin in environmental friendly ionic liquids. *J. Mol. Liq.* **2020**, *305*, No. 112854.

(44) Hanselmann, R.; Reeve, M. M. Crystalline Forms of D-Glucitol, 1-Deoxy-1-(Methylamino)-, 1-(6-Amino-3, 5-Difluoropyridine-2-Yl)-8-Chloro-6-Fluoro-1, 4-Dihydro-7-(3-Hydroxyazetidin-1-Yl)-4-Oxo-3-Quinolinecarboxylate. U.S. Patent US20160046603A1, 2016.

(45) Ramzan, M.; Yousaf, A. M.; Khan, I. U. Fabrication and in vitro characterization of delafloxacin-laden electrosprayed hydroxypropyl cellulose nanoparticulated solid dispersions for enhanced aqueous solubility and release rate of the drug. *Int. J. Polym. Mater. Polym. Biomater.* **2023**, *73*, 1367–1373.

(46) de Melo, L. P.; Salmoria, G. V.; Fancello, E. A.; Roesler, C. R. M. Effect of Injection Molding Melt Temperatures on PLGA Craniofacial Plate Properties during In Vitro Degradation. *Int. J. Biomater.* **2017**, *2017*, No. 1256537.

(47) EMEA. *Quofenix: International Non-Proprietary Name: Delafloxacin*; European Medicines Agency, Science Medicines Health: An Agency of the European Union: Neitherland, 2019, pp 1–123.

(48) Singh, G.; Kaur, T.; Kaur, R.; Kaur, A. Recent biomedical applications and patents on biodegradable polymer-PLGA. *Int. J. Pharmacol. Pharm. Sci.* **2014**, *1* (2), 30–42.

(49) Tripathi, A.; Gupta, R.; Saraf, S. A. PLGA nanoparticles of anti tubercular drug: drug loading and release studies of a water insoluble drug. *Int. J. Pharm. Tech Res.* **2010**, *2* (3), 2116–2123.

(50) Pfaller, M. A.; Flamm, R.; McCurdy, S.; Pillar, C.; Shortridge, D.; Jones, R. Delafloxacin in vitro broth microdilution and disk diffusion antimicrobial susceptibility testing guidelines: susceptibility breakpoint criteria and quality control ranges for an expanded-spectrum anionic fluoroquinolone. *J. Clin. Microbiol.* **2018**, *56* (8), No. e00339–18.

(51) Hines, D. J.; Kaplan, D. L. Poly (lactic-co-glycolic) acid–controlled-release systems: experimental and modeling insights. *Crit. Rev. Ther. Drug Carrier Syst.* **2013**, *30* (3), 257–276, DOI: [10.1615/CritRevTherDrugCarrierSyst.2013006475](https://doi.org/10.1615/CritRevTherDrugCarrierSyst.2013006475).

(52) Houchin, M.; Topp, E. Chemical degradation of peptides and proteins in PLGA: a review of reactions and mechanisms. *J. Pharm. Sci.* **2008**, *97* (7), 2395–2404.

(53) Makadia, H. K.; Siegel, S. J. Poly lactic-co-glycolic acid (PLGA) as biodegradable controlled drug delivery carrier. *Polymers* **2011**, *3* (3), 1377–1397.

(54) Friess, W.; Schlapp, M. Release mechanisms from gentamicin loaded poly (lactic-co-glycolic acid)(PLGA) microparticles. *J. Pharm. Sci.* **2002**, *91* (3), 845–855.

(55) Elsayed, M. M.; Elsayed, A.; Fouad, M.; Mohamed, M. S.; Lee, S.; Mahmoud, R. A.; Sabry, S. A.; Ghoneim, M. M.; Hassan, A. H.; Abd Elkarim, R. A.; et al. Development and optimization of vildagliptin solid lipid nanoparticles loaded ocuserts for controlled ocular delivery: A promising approach towards treating diabetic retinopathy. *Int. J. Pharm.: X* **2024**, *7*, No. 100232.

(56) Remy, J. M.; Tow-Keogh, C. A.; McConnell, T. S.; Dalton, J. M.; DeVito, J. A. Activity of delafloxacin against methicillin-resistant *Staphylococcus aureus*: resistance selection and characterization. *J. Antimicrob. Chemother.* **2012**, *67* (12), 2814–2820.

(57) DeLeo, F. R.; Chambers, H. F. Reemergence of antibiotic-resistant *Staphylococcus aureus* in the genomics era. *J. Clin. Invest.* **2009**, *119* (9), 2464–2474.

(58) Saravolatz, L. D.; Pawlak, J. M.; Wegner, C. Delafloxacin activity against *Staphylococcus aureus* with reduced susceptibility or resistance to methicillin, vancomycin, daptomycin or linezolid. *J. Antimicrob. Chemother.* **2020**, *75* (9), 2605–2608.

(59) Bulut, O.; Oktem, H. A.; Yilmaz, M. D. A highly substituted and fluorescent aromatic-fused imidazole derivative that shows enhanced antibacterial activity against methicillin-resistant *Staphylococcus aureus* (MRSA). *J. Hazard. Mater.* **2020**, *399*, No. 122902.

(60) Borah, P.; Hazarika, S.; Chettri, A.; Sharma, D.; Deka, S.; Venugopala, K. N.; Shinu, P.; Al-Shar'i, N. A.; Bardaweel, S. K.; Deb, P. K. Heterocyclic Compounds as Antimicrobial Agents. In *Viral, Parasitic, Bacterial, and Fungal Infections*; Bagchi, D.; Das, A.; Downs, B. W., Eds.; Academic Press, 2023; Chapter 61, pp 781–804.

(61) Abd El-Aleam, R. H.; George, R. F.; Hassan, G. S.; Abdel-Rahman, H. M. Synthesis of 1,2,4-triazolo[1,5-a]pyrimidine derivatives: Antimicrobial activity, DNA Gyrase inhibition and molecular docking. *Bioorg. Chem.* **2020**, *94*, No. 103411.

(62) Finch, R. G.; Greenwood, D.; Whitley, R. J.; Norrby, S. R. *Antibiotic and Chemotherapy e-book*; Elsevier Health Sciences, 2010.

(63) Pham, T. D. M.; Ziora, Z. M.; Blaskovich, M. A. T. Quinolone antibiotics. *Medchemcomm* **2019**, *10* (10), 1719–1739.

(64) Turban, A.; Guerin, F.; Dinh, A.; Cattoir, V. Updated Review on Clinically-Relevant Properties of Delafloxacin. *Antibiotics* **2023**, *12* (8), No. 1241, DOI: [10.3390/antibiotics12081241](https://doi.org/10.3390/antibiotics12081241).

(65) Li, Z.; Tao, W.; Zhang, D.; Wu, C.; Song, B.; Wang, S.; Wang, T.; Hu, M.; Liu, X.; Wang, Y.; et al. The studies of PLGA nanoparticles loading atorvastatin calcium for oral administration in vitro and in vivo. *Asian J. Pharm. Sci.* **2017**, *12* (3), 285–291.

(66) Park, T. G. Degradation of poly(lactic-co-glycolic acid) microspheres: effect of copolymer composition. *Biomaterials* **1995**, *16* (15), 1123–1130.

(67) Huang, W.; Zhang, C. Tuning the Size of Poly(lactic-co-glycolic Acid) (PLGA) Nanoparticles Fabricated by Nanoprecipitation. *Biotechnol J.* **2018**, *13* (1), No. 1700203, DOI: [10.1002/biot.201700203](https://doi.org/10.1002/biot.201700203).